MIXED MATRIX MEMBRANES COMPRISING GLASSY POLYMERS AND DISPERSED MESOPOROUS SILICA SPHERES FOR GAS SEPARATION

Beatriz Zornoza, Carlos Téllez*, Joaquín Coronas

Chemical Engineering Department and Nanoscience Institute of Aragón. Universidad de Zaragoza, 50018 Zaragoza, Spain

* Corresponding author:

Dr. Carlos Téllez Ariso

Chemical Engineering Department and Nanoscience Institute of Aragón

University of Zaragoza

Centro Politécnico Superior. c/ María de Luna, 3 50018 Zaragoza. Spain

Phone: 34 976 761000, Ext. 5429. Fax: 34 976 761879

e-mail: ctellez@unizar.es

ABSTRACT

Mixed matrix membranes (MMMs) composed of polyimide Matrimid® and mesoporous silica spheres (MSSs) are prepared, characterized and tested in gas separation of equimolar mixtures H_2/CH_4 and CO_2/N_2 at different temperatures. Its performance is compared with MMMs using other glassy polymer: polysulfone Udel®. The convenience of removing the structural agent from the pores and activate the mesoporous with calcination or chemical extraction have been studied. In both studied polymers, the permeability of the selective gas increases with the filler and the selectivity has a maximum at 8 wt % filler loading. These improvements are related with the mesoporosity of the filler, good interaction between the filler and the polymer, and change in the polymer structure as indicate the characterization done by thermogravimetric analysis, x-ray diffraction, differential scanning calorimetry, and scanning and transmission electron microscopy.

Keywords: Mixed matrix membranes, Gas separation, Mesoporous silica sphere, Polysulfone, Polyimide

1. INTRODUCTION

A polymer to be effective in gas separation processes has to comply with certain criteria: (1) must provide the ability to leave their gas molecules permeate through it, (2) must permit the separation of the desired gas in the membrane, and (3) must be chemically resistant, mechanical and thermally stable and include a high permeability (which determines the productivity) and high selectivity (high development of the material). Indeed these two gas transport parameters of the membrane material are the ones to eventually define the success of gas separation processes [1].

Robeson reported in 1991 [2] (and subsequently updated in 2008 [3]) that the performance of polymers is limited by an upper-bound trade-off line, which demonstrates a strong inverse relationship between the aforementioned parameters: permeability and selectivity (polymers that are more permeable are commonly less selective and vice versa). In order to improve performance, new materials and procedures for membrane fabrication are being investigated. While inorganic membranes [4] have been shown to have exceptional gas separation properties and endure high stability under temperature and hard physical and chemical environments, they also have elaborated manufacturing procedures with low reproducibility due to low mechanical resistance and breakability, high cost, and poor intensification. In contrast, polymer membranes demonstrate moderate separations under the upper-bound curve, but lower cost, easy manufacturing and higher mechanical properties. Therefore, the combination of the filler material with a polymer matrix could be an excellent proposal to overcome the limitations established by Robeson, while maintaining the mechanical flexible properties of the polymeric matrix. This alternative type of membrane material, which is known as mixed matrix membrane (MMM), has begun to catch the attention of many researchers. The formation of an inorganic-organic material with excellent

interfacial compatibility between phases is the most prominent challenge in hybrid membrane performance since the advantages of both phases are complemented each other [5,6]. However, the preparation of MMMs using glassy polymers as the continuous phase has been reported to be complicated due to the poor polymer-sieve contact in some cases [7]. Thus, in such hybrid material the effectively wetting of the polymer around the filler surface (avoiding the formation of non-selective voids at the polymer/filler interface) is clearly important to fulfil the selectivity enhancement and rise above the region of industrial attractiveness [2].

In this work ordered mesoporous materials embedded in glassy polymers were used. Glassy polymers often provide better transport performance for specific gas permeation mixtures comparing to rubbery materials, but have the difficulty of rigid chain mobility in the formation of the membranes which could cause interfacial gaps between the two phases[1,8,9]. Among this kind of polymers, polyimides and polysulfones represent an impressive potential in terms of its industrial viability due to their gas permeability and high intrinsic permselectivity coupled with excellent mechanical strength, high thermal stability, solvent resistance and commercial availability [10]. Consequently, a big effort to minimize the effect of the polymer chain mobility is needed. The use of mesoporous materials rather microporous ones could focus on achieving this challenge [11,12]. Thus, the adhesion of polymer chains to an embedded particle could be facilitated by the mesoporosity that could allow polymer chain penetration.

Since the discovery of M41S family in 1992 [13], a variety of ordered mesoporous materials have been synthesized with a vast range of framework compositions, morphologies, and pore structure. Ordered mesoporous silica materials have received a great deal of intensive research because its increasing industrial

applications such as catalysis supports, adsorbents, and membrane separations due to their unique properties such as high mechanic and thermal stability, facility of chemical functionalization, owing to reactive silanol groups, high specific surface areas (> 500 m^2), and well defined mesoporous array and porosity (bigger pores, 2-50 nm). Due to the mesoporosity of silica particles, and taking into account that the cross sectional areas per chain of the most selective synthetic polymers are around 1 nm^2 or less [14], the polymer could therefore be able to penetrate into the pores and enhance the contact.

In spite of the good adhesion to the polymer matrix, ordered mesoporous materials (i.e. MCM-41 and MCM-48) would offer some limitations concerning gas separation performance due to the gas transport trough the inorganic mesoporous membranes commonly follow the Knudsen diffusion model where the permeance is inversely proportional to the square root of molecular weight of the penetrants. However, in terms of interaction this strategy proved to be effective. When calcined mesoporous particles are embedded in polysulfone polymer matrix not only similar permselectivities to the bare membrane [15] due to the hydrogen bonding with the OH-rich surface of the mesoporous silica are managed but could be going above. This is a result of the selective diffusivity produced by the penetration of the polymer chain into the internal surface of the calcined siliceous material [12,16]. Thus, the large pores of this material may be easily blocked by the polymer chains leaving the inner pores inaccessible [17]. Even though permeabilities when increasing silica loading augment according to the gas transport properties dictated by the inorganic phase, the selectivities for the hybrid system could be still much higher than the ideal selectivities envisaged with the Knudsen model. In this way the interactions between the dense polymer matrix and the sieves in the hybrid membrane lead to the formation of selective channels, which show a prominent potential for gas separation processes [15,18].

In our previous work [12], mixed matrix membranes were prepared comprising polysulfone Udel® matrix and ordered mesoporous silica spheres as filler. Moreover, an optimum loading of 8 wt % was found in terms of H_2/CH_4 separation performance due to the interaction between the filler and the polymer. The research presented now focuses on the preparation and characterization of mixed matrix membranes including Matrimid® polyimide and calcined or chemically extracted mesoporous silica spheres (MSSs) as the molecular sieve inorganic phase. The permeability/permselectivity properties will be tested for the separation of H_2/CH_4 and CO_2/N_2 equimolar mixtures at different operating conditions of temperature and pressure. Besides, characterization measurements and permeation results of MMMs composed of Udel® will be compared with Matrimid®.

2. EXPERIMENTAL SECTION

2.1. Synthesis and characterization of mesoporous silica spheres (MSSs)

MSSs were prepared as described in the literature [19], but including slight variations in the molar composition of the synthesis [l,20] since the nature of the precursors and the relative compositions in the synthesis gel influence several properties of these materials such as superficial area, pore volume, unit cell parameter, pore diameter, and the silica wall thickness [21]. To prepare the MSSs used in this work a source of silica (sodium metasilicate, Na_2SiO_3, Sigma-Aldrich), a template (surfactant molecule) (cetyltrimethylammonium bromide (CTABr), $C_{19}H_{42}NBr$, Sigma-Aldrich), and an initiator for the particles formation (ethylacetate, $CH_3COOC_2H_5$, Sigma-Aldrich) were used. The chemicals were mixed in order to obtain a synthesis gel with the following molar composition: 1.5 Na_2SiO_3:1CTABr:361H_2O:7.4$CH_3COOC_2H_5$. Once mixed, the resulting sol was kept in a closed polypropylene flask at room temperature

for 5 h. The synthesis proceeded at 90 ºC for 50 h in the same open flask, without stirring. The final product was washed several times in distilled water and ethanol, and then filtered. Fig. 1 shows the SEM microphotograph of the mesoporous silica prepared here. It indicates that the diameter of the mesoporous silica is uniform with sizes between 2-4 µm, in agreement with previous works [20,22].

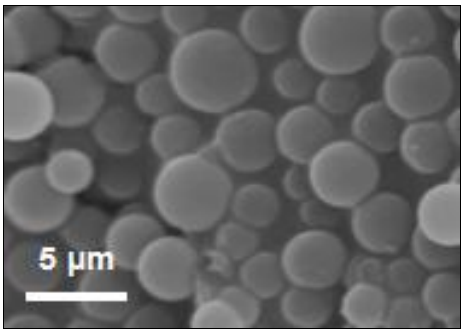

Fig. 1. SEM image of the prepared mesoporous silica spheres.

To remove the structural agent from the pores and activate the mesoporous structure of the MSSs, the final powder was subjected to two different treatments. In the first treatment, MSSs were calcined at 600 ºC for 8 h with heating and cooling rates of 0.5 ºC/min. In the second, the surfactant was removed through Soxhlet extraction using an ethanol/HCl/water mixture including 250 mL of ethanol and 9 g of HCl (37 wt %) per g of MSSs at 70 ºC for 15 h.

Low angle x-ray diffraction (LA-XRD) spectra of chemically extracted and calcined MSS were recorded on a Philips X'Pert diffractometer with Bragg-Brentano geometry and Cu Kα radiation (40 kV, 20 mA). Data were measured from $2\theta = 0.6^{o}$ to 8^{o} in steps of 0.02^{o} and t = 5 s/step.

Nitrogen adsorption-desorption isotherms of MSSs with and without directing agent were measured at 77K using a *porosity analyzer* (TriStar 3000, Micromeritics Instrument Corp.). The samples were outgassed with a heating rate of 10 ºC/min until

110ºC for as-synthesized MSSs and at 350ºC for extracted and calcined MSSs, and mantained for 8 h. BET specific surface areas were measured from the adsorption branches in the relative pressure range of 0.05-0.25 and the pore size distributions were calculated using the Barrett-Joyner-Halenda (BJH) model form the adsorption branches.

Thermogravimetric analyses were performed using Mettler Toledo TGA/SDTA 851^{e} equipment. Samples of MSSs (around 10 mg) were placed in 70 μL alumina pans and heated in air flow up to 600 °C at a heating rate of 5 ºC/min.

Fourier Transformed Infrared Spectroscopy (FTIR) through a Bruker Vertex 70 FTIR spectrometer was used to examine the presence of surface functional groups and the absence of the structure directing agent (CTABr) from the synthesis of the mesoporous silica particles. Samples of MSSs were prepared using the KBr wafer technique. The measures were done at different temperatures (110-400 ºC) in a diffuse reflectance module to avoid the interferences caused by the hydroxyl groups of water. Data were registered with OPUS software from Bruker Optics.

2.2. Preparation of Mixed matrix membranes (MMMs)

Flat polyimide Matrimid® (PI) 5218 and polysulfone Udel® P-3500 (PSF) membranes (kindly supplied by Huntsman Advanced Materials, and Solvay Advanced Polymers, respectively) were prepared to compare their gas separation performance with those of films containing increased amounts of MSSs (loadings of 4, 8, 12 and 16 wt %) as dispersed phase. Both amorphous hydrophobic polymers are soluble in several solvents and have excellent mechanical and thermal properties with a glass transition temperature above 315 ºC and 185 ºC, correspondingly.

Previous of the preparation of the MMMs, the polymeric matrix was dried overnight over vacuum at 100 ºC (for PSF membranes) and 150 ºC (for PI membranes)

to remove adsorbed moisture. The method for preparing the pure polymeric membranes consisted basically in dissolving the polymer (in a percentage of 90 wt %) in chloroform, allowing good viscosity of the casting solution. This percentage was kept constant for the MMMs. To fabricate MMMs, the synthesized MSSs were dispersed in chloroform (around 90 wt % of solvent-10 wt % inorganic filler-polymer mixture) in an ultrasonic bath for 15 minutes. The polymer proportion of PI or PSF was then added and the resulted dispersion was stirred magnetically at room temperature for 24 hours. Before the membrane casting three intervals of sonication of 15 min were carried on to guarantee a well-dispersed solution. Subsequently, the homogeneous solution was casted on a plain glass surface or Dr. Blade system and left overnight at room temperature to get natural evaporation. The last step was the vacuum treatment under 10 mbar of pressure to remove the solvent still remaining within the membrane. The treatment took place in a vacuum oven (Memmert) at 100 ºC for PSF and at 150 ºC for PI films, respectively. Membrane thicknesses (measured using a Digimatic Micrometer Quickmike, Mitutoyo Corp.) from 75-100 μm with different amounts of molecular sieve were performed. The average value of thickness of all membranes tested was 81 μm ± 8 μm. Membrane circles of about 15.2 cm^2 were cut from the films for permeation tests.

2.3. Techniques for membrane characterization

The *SEM images* were collected on a JEOL JSM 6400 scanning electron microscope (Jeol Corp.) operating at 20 kV. For this aim, cross sections were prepared by freeze-fracturing after immersion in liquid N_2. *TEM analysis* was also used to verify the good contact between both the dispersed MSSs and the continuous polymeric phase. In this technique a portion of the membrane was embedded in an Epofix™ cold-setting resin (Electron Microscopy Sciences). Then, 15 parts of embedding resin and 2 parts of hardener (in volume proportion) were mixed, while the curing time was 8 h at room

temperature, so that the cross section pieces could be sliced into the desired sections thin enough to be transparent for the electron beam. The slices were cut at 30-60 nm thickness using a RMC MT-XL ultramicrotome (RMC Products) with a Standard Ultraknife 45º, 3 mm diamond blade (Drukker Ultra-microtome knife). The sliced sections were stained in aqueous solution, placed on carbon copper grids and subsequently observed at 200 kV in a JEOL-2000 FXII TEM (Jeol Corp.)

Thermogravimetric analyses (TGA) were performed using a Mettler Toledo TGA/SDTA 851^e instrument. Samples were heated in air flow up to 850 °C at 10 ºC/min maintaining the final temperature for 1 h. *Differential scanning calorimetry (DSC)* measurements were proceeded using a Mettler Toledo DSC822^e equipment to estimate the glass transition temperature (T_g) of the MMMs with growing percentages of MSSs. Small pieces of dried membranes were transferred to 40 μL aluminum pans, which were hermetically sealed with aluminum covers. The samples were first scanned from room temperature to 400 ºC with heating rate of 20 ºC/min. Two consecutive runs of this method were performed for each sample and the glass transition temperature (T_g) was calculated from the middle point of the slope transition in the DSC curve. The reported Tg values are the average value based on the second runs of at least three samples.

Mixed matrix membranes were moreover characterized by *X-ray diffraction (XRD)* using a D-Max Rigaku X-ray diffractometer with a copper anode and a graphite monochromator to select $CuK_{\alpha 1,2}$ radiation (λ = 1.540 Å). Data were measured from 2θ = 2.5º to 40º in steps of 0.03º and t = 1 s/step.

2.4. Permeability measurements

The membranes were tested in a gas permeation setup [12] to separate 50% binary mixtures of both H_2/CH_4 and CO_2/N_2. The feed mixtures, separately, entered by the retentate side of the membrane through two Alicat Scientific mass-flow controllers (global flow of 50 cm^3(STP)/min)) at different pressures above the atmospheric one (275 and 400 kPa). The membranes were hold into a permeation module which consists of two stainless steel pieces with a cavity to place additionally a macroporous disk support 316LSS with 20 μm nominal pore size (Mott Corp.) and gripped Viton® o-rings. The permeate side of the membrane was swept with a 1 cm^3(STP)/min mass-flow (Alicat Scientific) controlled stream of Ar at atmospheric pressure, allowing the transport of gases due to the created different partial pressure. When the CO_2/N_2 mixture was tested, He was used as the sweep gas (5 cm^3(STP)/min). The outgoing concentrations of H_2/CH_4 and CO_2/N_2 were analyzed by an on-line gas micro-chromatograph (Agilent 3000A) equipped with TCD. Permeability results were obtained when the exit stream of the membrane was stabilized. The real separation selectivity of both mixtures was calculated as the ratio of experimental permeabilities. Permeabilities are presented in Barrer units (1 Barrer = $1 \cdot 10^{-10}$ cm^3(STP)·cm/(cm^2·s·cmHg)). The permeation measurements were performed at different temperatures: 35, 60, and 90 ºC controlled by an oven (Memmert). Thus, apparent activated energies for the membranes with increasing loading of calcined MSSs within the polymer matrix were obtained.

3. RESULTS AND DISCUSSION

3.1. Surfactant removal

Fig. 2 depicts FTIR spectra of as-made MSSs and MSSs after the surfactant was removed by calcination or Soxhlet extraction using ethanol/HCl mixture. The FTIR

spectra of as made MSSs shows peaks at around 574 cm^{-1} (distortion of the Si-O tetrahedrons), 805 cm^{-1} (Si-O-Si bending), 973 cm^{-1} (internal Si-OH) and 1073 cm^{-1} (Si-O-Si stretching) corresponding to the SiO_2 characteristic bands due to the vibrations of Si–O–Si bridges crosslinking the silicate network [23]. As expected, as-synthesized MSSs (curve a) present absorption peaks in the range of 3000-2850 cm^{-1} and around 1400 cm^{-1}, corresponding to C-H bending and C-H stretching, respectively, of the surfactant carbon structure. From chemically extracted MSSs (curve b) it can be also depicted these adsorption branches. However, the intensity is much lower indicating that the majority of surfactant has been removed. The bands corresponding to surfactant are not evident in the calcined sample indicating the completely removal of the surfactant.

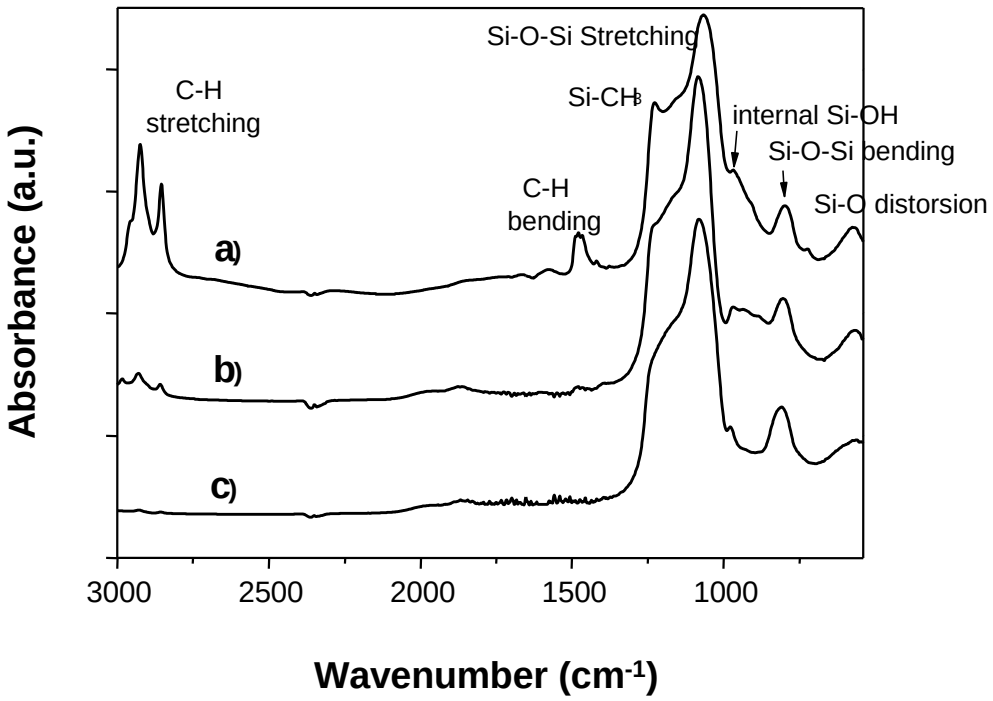

Fig. 2. FTIR spectra of: a) as-made MSSs at room temperature, b) chemically extracted MSSs at 110 ºC, c) calcined MSSs at 110.

To corroborate and quantify the presence of surfactant, TGA analyses have been performed (Fig. 3). The MSSs without removal of the template show around 4% weight

loss below 100 ºC, associated with physically adsorbed water, and around 40% weight loss over 150 ºC, associated with surfactant decomposition. TGA results of calcined sample indicated that the CTABr surfactant was completely removed by this procedure. Instead, the chemically extracted sample shows a weight loss about 3% related to the remaining surfactant in consistent with FTIR results.

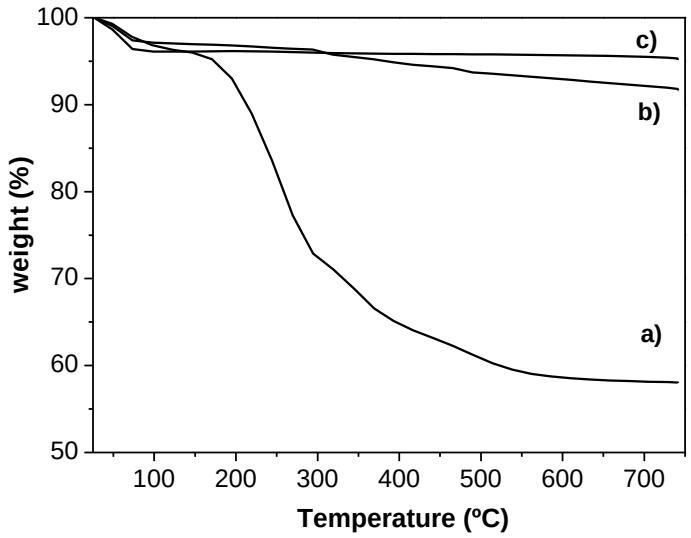

Fig. 3. TGA weight losses versus temperature for a) as-made MSSs, b) chemically extracted MSSs, c) calcined MSSs.

Low angle X-ray diffraction performed in calcined MSSs (Fig. 4) displayed a strong reflection at 2.42º and two weak reflections at higher 2·θ corresponding to (100), (110) and (200) planes indicating that this material has a pore structure of hexagonal in nature [23] that can be attributed to MCM-41 pores. The position of the first (100) peak at 2·θ = 2.42º gives the repetition spacing of the pores d_{100}= 3.65 nm by the Bragg's law. The chemically extracted sample has the same peaks but with lower intensity. The first peak at 2·θ = 2.17º corresponds to a d_{100}=4.1 nm. These results indicate the unit cell shrinkage upon calcination respect the chemically extracted sample where some surfactant remains.

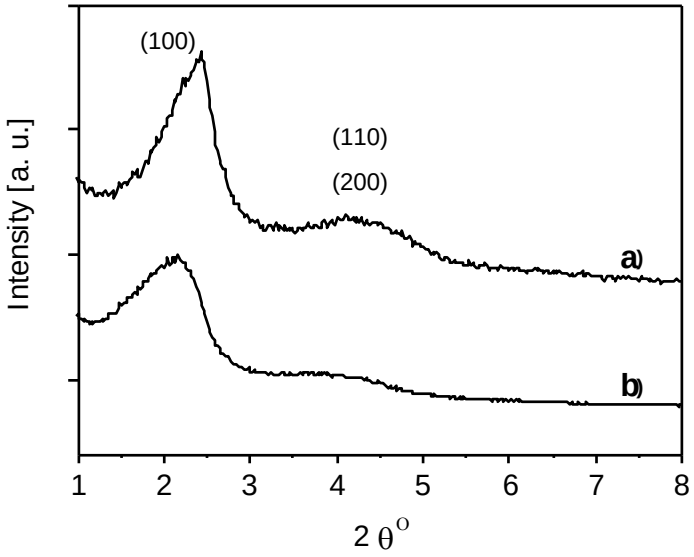

Fig. 4. Low angle X-ray diffraction of MSSs: a) calcined b) chemically extracted.

Fig. 5 shows the N_2 adsorption/desorption type IV isotherms for the calcined MSSs and chemically extracted MSSs. The calcined sample showed a bimodal pore-size distribution with sharp peak at 2.7 nm that correspond to MCM-41 pores observed by low XRD and abroad peak around 9 nm corrrespondig to non MCM-41 pores (pore-size distributions were calculated using the adsorption branch of the N_2 adsoprtion/desorption isotherm and the Barret-Joyner-Halenda (BJH) method). The BET surface area was 1023 m^2/g. The bimodal pore system for MSSs spheres has been previously reported [19,20].

For the chemically extracted MSSs, there is also a bimodal pore-size distribution with slightly changes in the values for both kind of pores (2.3 nm for the first peak and 16 nm for the second peak). It is more noticeable, the change on the BET surface area which is 851 m^2/g for the sample chemically extracted. These decreases respect to the calcined sample are related to remaining surfactant inside the pores mainly in the small pores (see inset of Fig. 5). Considering the BET surface area of calcined sample the real

surface of MSSs (all the surfactant is removed as the TGA analyses indicated) the opened mesoporosity in the chemical extracted MSSs would be about 83%.

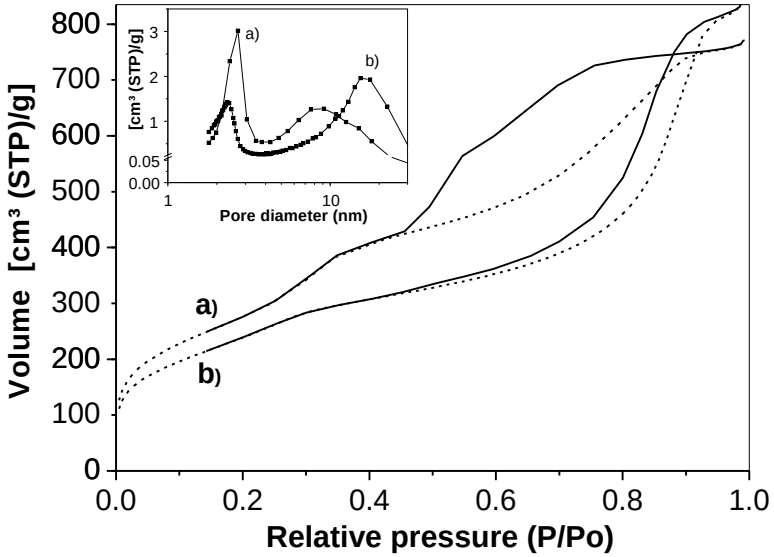

Fig. 5. Nitrogen adsorption (dotted lines) and desorption (solid lines) isotherm branches for: a) calcined MSSs, b) chemically extracted MSSs. The inset represents the pore size distribution for calcined and extracted MSSs, respectively.

3.2. Characterization of mixed matrix membranes (MMMs)

The dispersion of the 8 wt % mesoporous silica spheres (calcined and chemically extracted) within the polymer (PSF and PI) in a MMMs is showed in the cross-sectional SEM micrographs of Fig. 6. In both polymers, the filler distribution is homogeneous, without apparent segregation and no agglomeration of the spheres are presented. Same behavior was found (not shown) with the other loadings varying between 0 and 16 wt %. The use of spheres in the form of 2-4 μm minimizes agglomeration and improves dispersibility because the spherical shape limits the contact between silica particles and the sphere size provides a lower external surface area to volume ratio than that used in other reports (MCM-41[15,18] or MCM-48 [28]).

Fig. 6, and more clearly its insets, shows the difference in adhesion between the particles and the polymer. The calcined samples are completely surrounded by the polymer, while the extracted samples show some voids. TEM images of MMMs with PI (Fig. 7) corroborate the good contact between the polymers and the calcined ordered silica, suggesting good affinity between the filler and the polymer, as happened with polysulfone [12]. The result suggests that polymer chains are able to penetrate into the mesopores of calcined MSSs, while the chemically extracted samples have some surfactant molecules in the pores plugging partially the entrance.

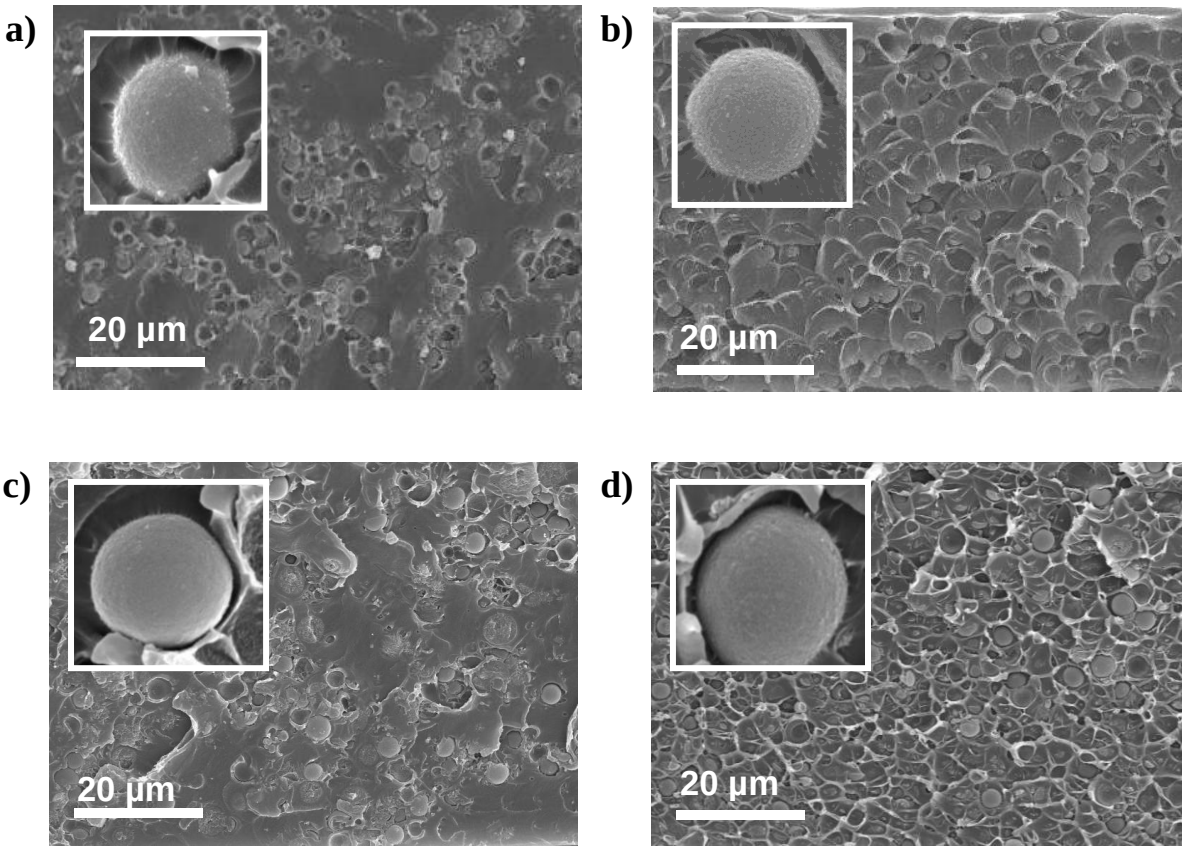

Fig. 6. Cross section SEM images of MMMs containing 8 wt % calcined MSS in: a) polysulfone matrix, b) polyimide matrix and 8 wt % chemically extracted MSS in: c) polysulfone matrix, d) polyimide matrix.

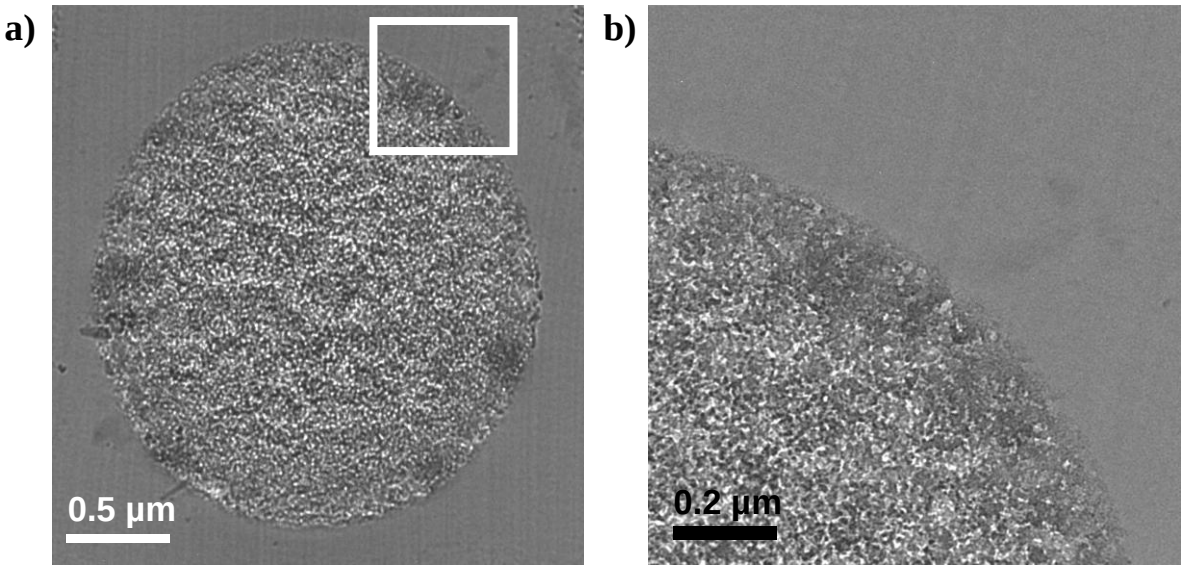

Fig. 7. TEM image of a): a calcined MSS within PI phase, b) detail of a)

X-ray diffraction (XRD) analysis (table 1) was used to study the arrangement of polymer chains of bare polymer and MMMs with 16 wt % calcined MSSs. The PSF and PI show inter-chain spacings of 0.52 nm and 0.62 nm, respectively. These inter-chain spacings are in agreement with the ones reported for PSF (0.50 nm) [24] and PI (0.58 nm) [25], both measured by X-ray diffraction. It can be seen that the inter-chain spacing of mixed matrix membranes is slightly reduced with the addition of calcined MSSs as has been observed for other fillers [25]. This may imply the tightening of polymer chains due to MSSs are closely integrated with the PI and PSF matrices according to microscopy images.

The glass transition temperature (Tg) gives a qualitative idea of the flexibility of polymer chains. In a previous article [12] Tg has been measured for bare PSF and MMMs of PSF+MSSs. There was a continuous increase in Tg as the MSSs mass fraction increased, namely, a 7.5 ºC difference: from 188.5 ºC at 0 wt % to 196 ºC at 16 wt %. It can be seen that the pure PI polymer (table 2) shows the Tg at 316.7 ºC, in agreement with the literature [26]. In case of MMMs using PI, the trend with MSSs is

the same as for PSF MMMs and the difference is slightly higher 27 ºC: from 316.7 ºC at 0 wt % to 343.8 ºC at 16 wt %. These results are consistent with increasing rigidity and restricted motion of the polymer chains due to the chemical interactions established between chain polymer and MSS mesoporosity. An analogous Tg variation has been reported for polyimide using other similar fillers [26].

Thermogravimetric analyses of bare PI (Fig. 8) show that there was no loss of weight up to 400 ºC indicating that solvent was removed with the vacuum treatment at 150ºC. Above this temperature, the decomposition of PI polyimide starts with a first peak of decomposition with a maximum at around 520 °C which could be attributed to a first degradation of the polymer, while H_2, CO, CO_2, and CH_4 light gases evolve from the sample [10]. There is a second peak of weight loss with a maximum at around 630 ºC. This is a consequence of the complete degradation of the polymer chain including the remaining carbon and residual non-elementary carbon components primarily N. For MMMs of PI, there was no weight loss up to 400 ºC indicating that solvent was removed and not trapped in the pores of the MSSs. In this sample, similar to bare polymer, there are two peaks of weight loss. It is noticeable the slight delay in the first peak and more clearly the second peak where the maximum temperature increases with the MSSS loading. That could be related to the interfacial interaction and the physical interpenetration around the boundary phase of polymer and filler [27]. The remaining weight loss allows the verification of the nominal wt % loading of inorganic filler present in the corresponding MMM, i.e., 0, 5.5, 10.6, and 16.8 wt % residual contents for nominal 0, 4, 8 and 16 wt %, respectively.

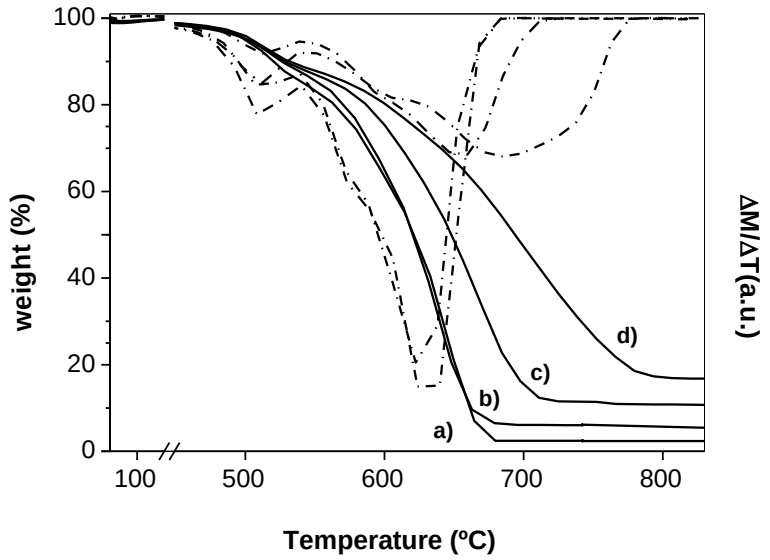

Fig. 8. TGA loss weight and its derivatives versus temperature for 0, 4, 8 and 16 wt % of calcined MSS in PI matrix (curves a), b), c) and d), respectively).

3.3. Gas separation measurements

Influence of loading

Fig. 9 shows the results of permeability and selectivity of mixed matrix membranes prepared from MSS-PSF and MSS-PI with 0-16 wt % loading for equimolar H_2/CH_4 mixture at 35 ºC. The data in this figure represent the average values of at least three membranes and error bar corresponds to standard deviation. The permeability for both gases and the H_2/CH_4 selectivity is higher in bare PI than bare PSF as can be also seen in table 3. For both polymers, H_2 and CH_4 permeabilities increase with filler loading and the H_2/CH_4 selectivity reaches a maximum at 8 wt %. In this filler loading, the PSF membrane permeabilities of hydrogen and methane were 26.5 and 0.34 Barrer, respectively, and the selectivity 79.2. Nevertheless, the PI mixed matrix membrane reached a permeability of hydrogen and methane of 46.9 and 0.29 Barrer, respectively, with a selectivity of 164.4.

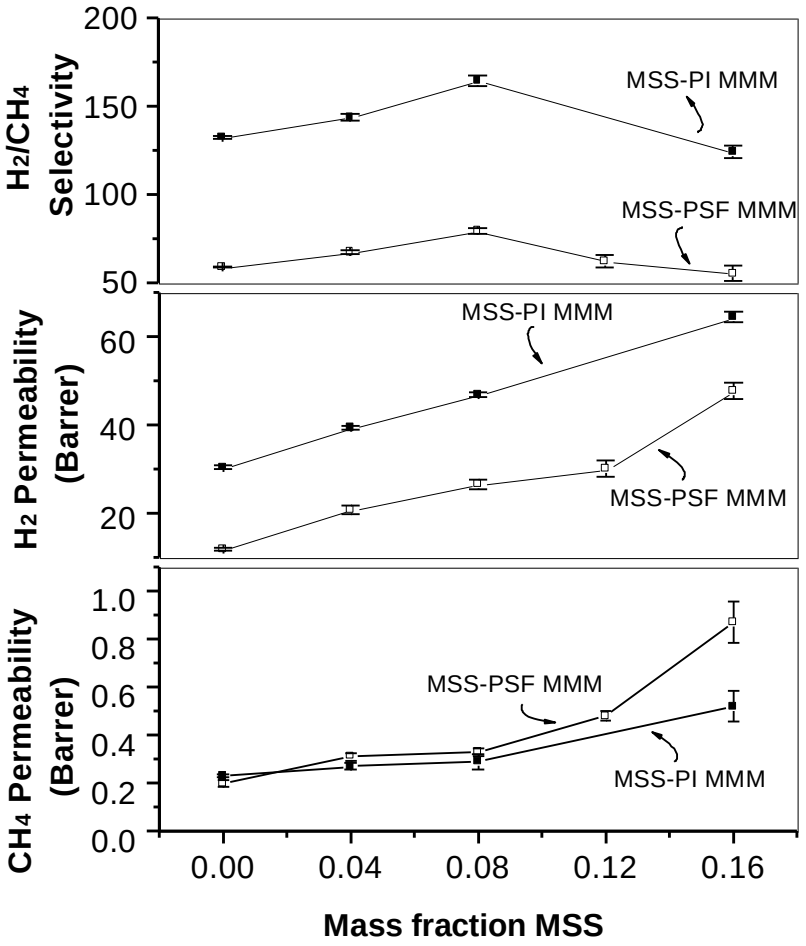

Fig. 9. Gas permeation results for calcined MSS-PSF/PI with loadings in the range of 0-16 wt % for the equimolar mixture H_2/CH_4 tested at 35 ºC and ΔP=175 kPa. The data are average values of at least three membranes and error bar corresponds to standard deviation.

The increase in permeability with loading could be explained taking into account a combination of two factors [28]: difference of permeability between filler and polymer and changes induced by the filler in polymer structure. The first factor is that gas transport can occur through the mesopores of silica spheres which is typically Knudsen flow, then the MSSs have a higher permeability than the polymer phase. As the filler for this study is in the M41S family, some permeability values of mesoporous silica membranes can be found in the literature [29,30,31]. An average value of this reference for hydrogen permeability would be 20000 Barrer, much higher than those of the bare PSF and PI polymers. Gas transport permeation properties in mixed matrix membranes

can be predicted using a model adapted from Maxwell's work or Lewis Nielsen model [32]. Both models predict clearly in this case an increase of the permeability when the MSSs are loaded in the polymer. The second factor has been explained in the literature as the disruption of polymer chain packing in the presence of silica particles [33,34] and/or changes which may be induced the silica filler in the organic/inorganic interphases [35]. This could be in agreement with the structural changes observed in the polymer ones characterized the PSF and PI using Tg, thermogravimetric analysis and d-spacing and the good contact observed with microscopy images. In addition, the rigidity increase of the polymer matrix could be responsible for the selectivity improvement as has been pointed out previously [12,33,35]. The loss of selectivity at higher MSS loadings (12-16 wt %) could be due to the generation of small non-selective voids existing between silica particles.

It should be noted that in our study a lower percentage of filler is used than in other works related to mesoporous molecular sieve fillers of the M41S family with loadings in the 10-40 wt % range. The low filler percentage implies less cost of inorganic material and less influence in the polymer mechanical properties.

Table 3 compares the performance on H_2/CH_4 separation of MMMs prepared with calcined and chemically extracted MSSs. The permeability of chemically extracted sample is slightly higher than that of the calcined sample, while the corresponding selectivities are lower. This is an expected behaviour due to the poor contact between polymer and MSSs. It is consistent with the formation of non-selective voids at the polymer-filler interface where viscous flow may occur. In fact, it should be noted that the performance of chemically extracted sample improves the bare polymer and could be a less energetically costly alternative (an also a more environmentally sensitive option) to calcined sample taking into account that the calcinations step is avoided.

Equimolar CO_2/N_2 mixtures have been also tested at 35 ºC (Fig. 10). Similar to H_2/CH_4 mixtures, the permeabilities of both gases and CO_2/N_2 selectivity are higher for the bare PI than for the bare PSF and the permeabilities for MMMs increased with filler loading reaching a maximum CO_2/N_2 selectivity with 8 wt % loading. The most remarkable difference between both mixtures is that the increase in selectivity with the filler loading is much higher with CO_2/N_2 mixture than with H_2/CH_4 mixture. For example, from pure PI polymer to 8 wt % MSS- PI MMMs the CO_2/N_2 selectivity increases from 26.6 to 40.3, while the H_2/CH_4 selectivity increases from 132.4 to 164.4.

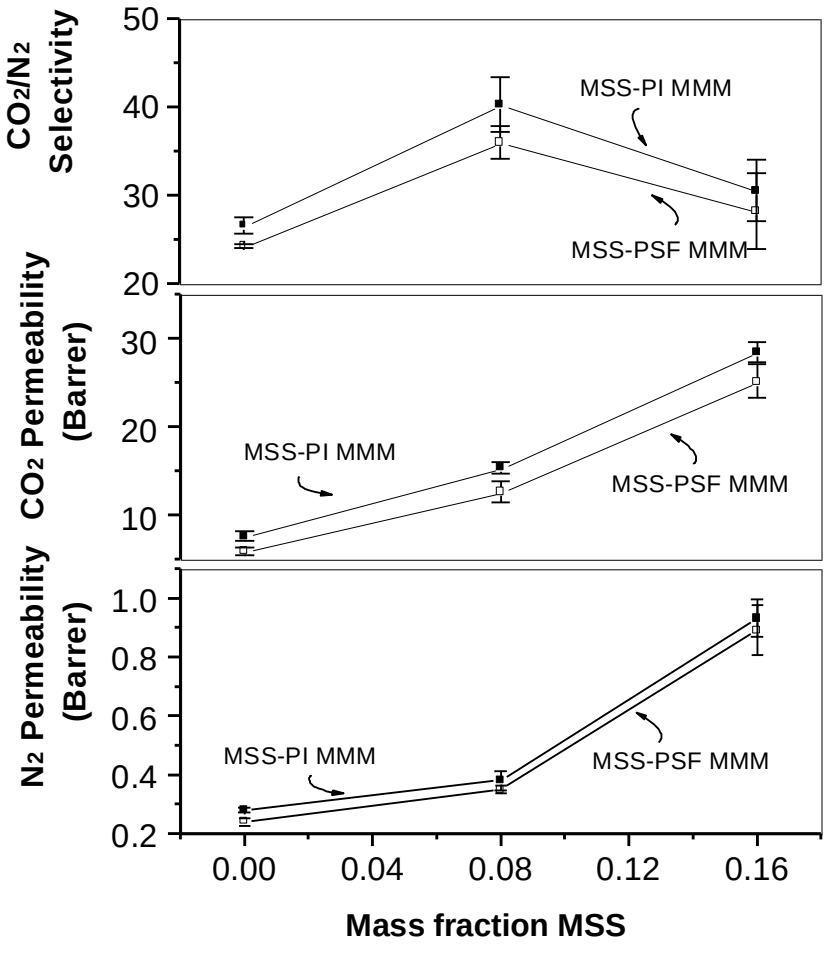

Fig. 10. Gas permeation results for calcined MSS-PSF/PI with loadings in the range of 0-16 wt % for the equimolar mixture CO_2/N_2 tested at 35 ºC and ΔP=175 kPa.. The data are average values of at least three membranes and error bar corresponds to standard deviation.

The same explanations set out in the case of the H_2/CH_4 mixture will be responsible of the behaviour observed in CO_2/N_2 mixture. In addition, it should be taken into account the nature of the separation of CO_2/N_2 where in porous materials the adsorption can play an important role. It should be taken into account the adsorpion capacity of the ordered mesoporous silicas (OMS) with uniform pore structure and high density of silanol groups (e.g. CO_2/N_2 selectivity of 8.6–22.2 for MCM-41 has been found [36] which is higher than Knudsen diffusion based selectivity). Besides, it could be considered that the structural change produced in the polymer by the filler could improve the polymer CO_2 adsorption.

Influence of temperature and pressure

Fig. 11 illustrates the effect of varying feed temperatures (35, 60, and 90ºC) and feed pressures (275 and 400 kPa) on H_2/CH_4 selectivity versus H_2 permeability values, for MMMs with 0, 4, 8, and 16 wt % MSSs within PSF and PI matrices. It can be observed that H_2 permeabilities (and CH_4 permeabilities, not shown in the graph) follow typical activation diffusion behaviors. The increase in temperature leaded to higher permeabilities, while this effect is more pronounced for MSS-PSF MMMs than for MSS-PI MMMs. When the operating temperature changes from 35 to 90 ºC the gas permeability of H_2 increased nearly 265% for 8 wt % MSS-PSF MMMs and 150 % for 8 wt % MSS-PI MMMs, respectively. For CH_4 gas permeability the improvement was just about 590% and 400% for both aforementioned membranes while declining the selectivity to the half. This behavior is consistent until 8 wt % filler charge. For the highest loadings, permeabilities augment reducing selectivity as has been explained previously.

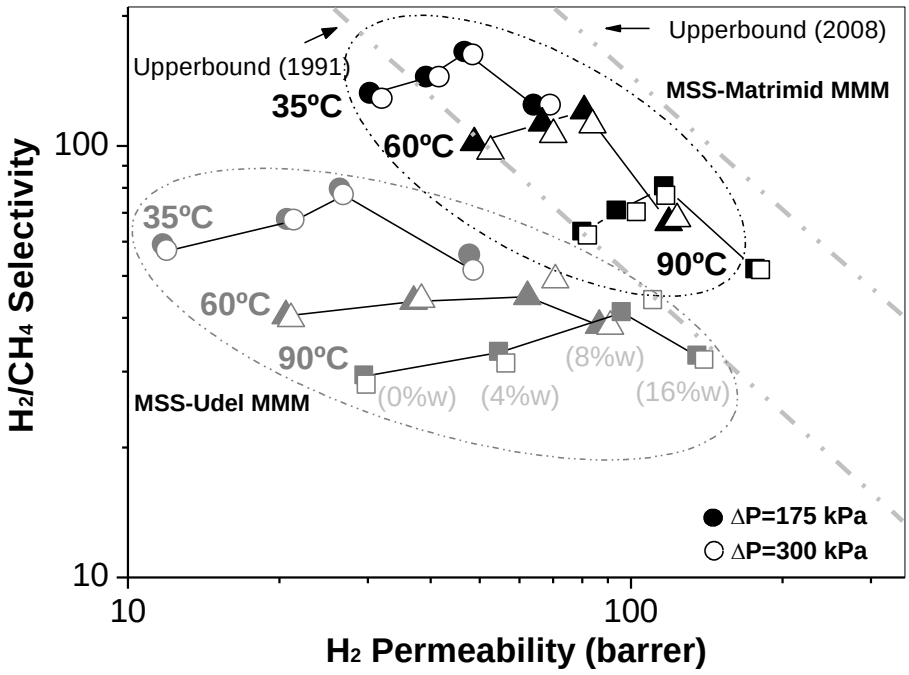

Fig. 11. Results for H_2/CH_4 at different pressures (ΔP of 175 kPa (closed symbols) and 300 kPa (open symbols)) and temperatures (at 35º C (circles), 60º C (triangles) and 90º C (squares)) within the Robesons'upper bound for MMMs composed of calcined MSS-PSF (0, 4, 8 and 16 wt %) and calcined MSS-PI (0, 4, 8 and 16 wt %).

Fig. 11 shows a typical Arrhenius relation (the higher the temperature, the higher the permeability). It should be reminded that membrane permeability (P) is the well-known product of the diffusion coefficient (D) and the solubility (S). The solubility decreases usually with the temperature but the diffusion coefficient increases. We observe an increase in permeability with temperature increase for all membranes and gases. Higher temperatures enhance the gas flux due to the promoted motion and flexibility of polymer chains, and thus the diffusivity of the penetrate gases is increased. On the contrary, an increase in temperature exhibits a decrease in permselecitivity since the increment in temperature increases the free volume of the membrane. Thus, the transport of both gases is improved. These trends with the temperature indicated that the solubility has a small influence on the process.

H_2 and CH_4 permeabilities did not change with feed pressure since adsorption is not so relevant is gas transportation as diffusion. These permeabilities presented a standard deviation less than 3% as the feed pressure augmented from 275 to 400 kPa (Note that the permeate pressure is the atmospheric).

With the optimum filler loading for H_2/CH_4 mixture (MMM of 8wt%MSS-PSF matrix) the Robeson's 1991 upper bound is achieved when increasing the temperature until 90 ºC, while results for 8 wt%MSS-PI MMMs approached to Robeson's 2008 upper bound at around 60º C and 90º C (Fig. 11).

The effect of the temperature (35, 60, and 90ºC) on CO_2/N_2 selectivity and CO_2 permeability values for MMMs with 0, 8, and 16 wt % MSSs within PI matrix is showed in Fig. 12. It should be noted that the working pressure is far away from the plasticization pressure (12 bar for PI and 34 bar for PSF [37]). Trends with temperature are similar to those observed for H_2/CH_4 mixture and the same explanations are applicable. The relations between permeability and selectivity for the CO_2/N_2 mixture (Fig. 12) are located below the Robeson upper bound (2008) when increasing temperature. To overcome the commercial attractive region of this actual Robeson´s upper bound is a challenge since the polymers used to calculate the curve have numerous modifications. Thus, with the use of that kind of polymers matrix with embedded MSSs, would be possible to manage the industrial region.

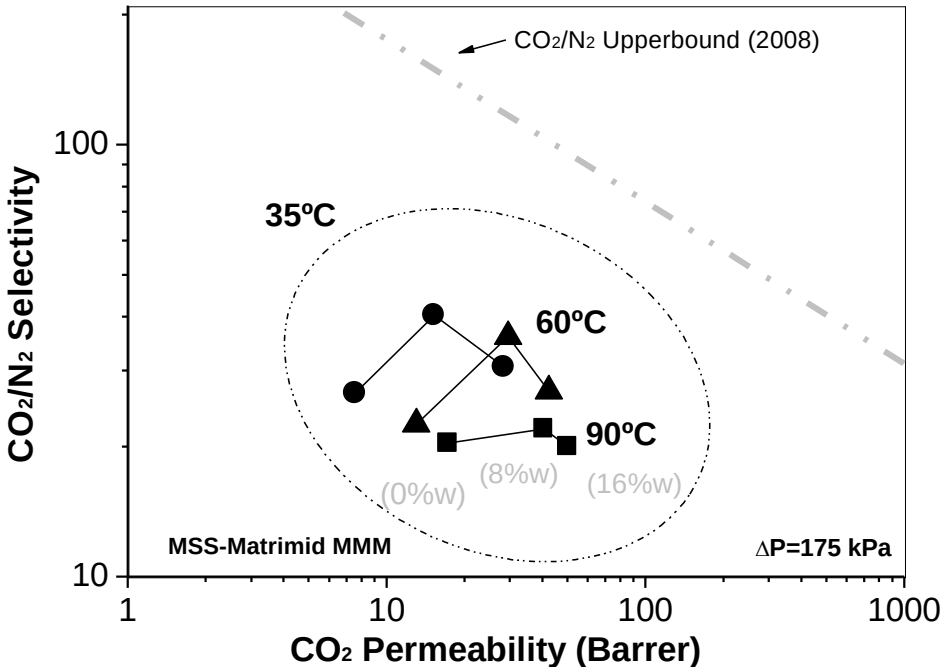

Fig. 12. Results for CO_2/N_2 at fixed pressure and different temperatures (35º C (circles), 60º C (triangles) and 90º C (squares)) and ΔP=175 kPa within the Robesons´upper bound for calcined MSS-PI MMMs (0, 8 and 16 wt %).

In order to explore the temperature dependence of H_2, CH_4, CO_2 and N_2 permeabilities in the membranes tested in this work, resulting data were correlated with the Arrhenius equation. This equation is used to correlate permeability/flux and temperature. Therefore, the activation energy of permeability (E_P) can be determined by using the Arrhenius expression:

$$P = P_0 \exp^{(-E_P / RT)}$$

where P is the permeability of the gas, P_0 is the pre-exponential factor (independent of temperature) with the same units as the permeability (Barrer), R is the universal gas constant and T is the absolute temperature.

Table 4 shows the apparent activated energies of the different MSS loading membranes for the gases tested in this work. The behaviour of E_P of the gases is typically governed by two main factors: molecular size and interaction with the polymer

(solubility) [38]. Gases that present low E_P values, such as H_2 and CO_2, exhibit a high permeability. However, higher E_P values were observed for N_2 and CH_4, the two least permeable gases. Moreover, the dependence of perselectivity with temperature has been observed to be larger for gas pairs with the difference in activation energies [39]. Finally, the estimated permeation activation energy for the four gases studied is higher for the MMMs membranes than for bare polymer membrane. This increase in activation energy permeation may also prove the chain rigidification in the MMMs [33].

4. CONCLUSIONS

The removal of the structural agent from the bimodal pores of ordered mesoporous silica spheres (MSSs) has been performed either using calcination at 600 ºC for 8 h or liquid phase extraction using an ethanol/HCl/water mixture at 70 ºC for 15 h. The calcination method activates the mesoporosity of MSSs removing completely the surfactant as TGA and FTIR analyses indicate. The chemical extraction method removes almost completely the template from the MSS spheres remaining surfactant mainly inside the MCM-41 pores.

A series of mixed matrix membranes were prepared comprising a glassy polymer (PSF or PI) matrix and MSSs as filler with loadings varying between 0 and 16 wt %. For both polymers, the scanning and transmission electron microscopy shows a good dispersion of the filler without agglomeration in the polymer matrix suggesting intimate interaction between the polymer and the filler. When the chemically extracted MSSs are used the interaction worsens.

There are several evidences of change in polysulfone and polyimide structures with the addition of MSSs: a) TGAs indicates a delay in the polymer degradation, b) XRD shows a reduction of inter-chain spacing of polymer chains, and c) DSC reveals an increase of the glass transition temperature. This is related to increasing rigidity and

restricted motion of the polymer chains due to the chemical interactions established between chain polymer and MSS mesoporosity.

The loading filler increases the permeability of the selective gas (H_2 and CO_2) and the H_2/CH_4 and CO_2/N_2 selective pass through a maximum at loading of 8 wt %. This behaviour is a consequence of the combination of two factors: (a) the high permeability of the filler compared to the polymer, and (b) changes induced by the filler in the polymer structure, as evidenced by several characterization techniques. An optimum loading of 8 wt % was found in terms of separation performance while higher loadings create voids between particles. At 35 ºC, with the optimum loading PSF MMMs were able to separate an equimolar H_2/CH_4 mixture with H_2 permeability= 26.5 Barrer and H_2/CH_4 selectivity= 79.2 and an equimolar CO_2/N_2 mixture with CO_2 permeability= 12.6 Barrer and CO_2/N_2 selectivity=36.0. With the optimum loading for PI MMMs, H_2 permeability= 46.9 Barrer and H_2/CH_4 selectivity= 164.4 and CO_2 permeability= 15.3 Barrer and CO_2/N_2 selectivity= 40.3 were registered.

The selectivity of chemically extracted MSSs sample is slightly lower than that of the calcined MSSs membrane, while the corresponding permeability is higher. In any event, chemically extracted MSSs improve the bare polymer and could be an energetically cheaper alternative.

In pure polymer and mixed matrix membranes, the increase of temperature produces an increase of permeability and a decrease of selectivity related to increased motion and flexibility of polymer chains, and thus the increase of diffusivity of the gases. The influence of pressure in the studied range is negligible. Finally, the permeation activation energies for H_2, CH_4, N_2 and CO_2 molecules increase when the MSSs are added to the polymer in accordance with the polymer chain rigidification.

ACKNOWLEDGEMENTS

Financial support from the Spanish Science and Innovation Ministry (MAT2007-61028, CIT-420000-2009-32) and the Aragon Government (PI035/09) is gratefully acknowledged. B. Z. also acknowledges the funding from the Spanish Ministry of Education and Science (FPU program) and Fundación Ibercaja.

REFERENCES

[1] R. Mahajan, D.Q. Vu, W.J. Koros, Mixed matrix membrane materials: An answer to the challenges faced by membrane based gas separations today?, J. Chin. Inst. Chem. Eng. 33 (2002) 77-86.

[2] L.M. Robeson, Correlation of separation factor versus permeability for polymeric membranes, J. Membr. Sci. 62 (1991) 165-185.

[3] L.M. Robeson, The upper bound revisited, J. Membr. Sci. 320 (2008) 390-400.

[4] J. Coronas, J. Santamaria, State-of-the-art in zeolite membrane reactors, Topic Catal. 29 (2004) 29-44.

[5] T.T. Moore, R. Mahajan, D.Q. Vu, W.J. Koros, Hybrid membrane materials comprising organic polymers with rigid dispersed phases, AIChE J. 50 (2004) 311-321.

[6] T.S. Chung, L.Y. Jiang, Y. Li, S. Kulprathipanja, Mixed matrix membranes (MMMs) comprising organic polymers with dispersed inorganic fillers for gas separation, Prog. Polym. Sci. 32 (2007) 483-507.

[7] R. Mahajan, W.J. Koros, Factors controlling successful formation of mixed-matrix gas separation materials, Ind. Eng. Chem. Res. 39 (2000) 2692-2696.

[8] D.Q. Vu, W.J. Koros, S.J. Miller, Mixed matrix membranes using carbon molecular sieves - II. Modeling permeation behavior, J. Membr. Sci. 211 (2003) 335-348.

[9] C.M. Zimmerman, A. Singh, W.J. Koros, Tailoring mixed matrix composite membranes for gas separations, J. Membr. Sci. 137 (1997) 145-154.

[10] J.N. Barsema, S.D. Klijnstra, J.H. Balster, N.F.A. van der Vegt, G.H. Koops, M. Wessling, Intermediate polymer to carbon gas separation membranes based on Matrimid PI, J. Membr. Sci. 238 (2004) 93–102.

[11] R.F. Boyer, R.L. Miller, Polymer-chain stiffness parameter, sigma, and cross-sectional area per chain, Macromolecules 10 (1977) 1167-1169.

[12] B. Zornoza, S. Irusta, C. Tellez, J. Coronas, Mesoporous silica sphere-polysulfone mixed matrix membranes for gas separation, Langmuir 25 (2009) 5903-5909.

[13] J.S. Beck, J.C. Vartuli, W.J. Roth, M.E. Leonowicz, C.T. Kresge, K.D. Schmitt, C.T.W. Chu, D.H. Olson, E.W. Sheppard, S.B. McCullen, J.B. Higgins, J.L. Schelenker, A new family of mesoporous molecular-sieves prepared with liquid-crystal templates, J. Am. Chem. Soc. 114 (1992) 10834-43

[14] G.C. Ruben, W.H. Stockmayer, Evidence for helical structures in poly(1-olefin sulfone)s by transmission electron-microscopy, Proc. Natl. Acad. Sci. U.S.A. 89 (1992) 7991-7995.

[15] B.D. Reid, A. Ruiz-Trevino, I.H. Musselman, K.J. Balkus, J.P. Ferraris, Gas permeability properties of polysulfone membranes containing the mesoporous molecular sieve MCM-41, Chem. Mater. 13 (2001) 2366-2373.

[16] S. Shu, S. Husain, W.J. Koros, A general strategy for adhesion enhancement in polymeric composites by formation of nanostructured particle surfaces, J. Phys. Chem. C 111 (2007) 652-657.

[17] E.V. Perez, K.J. Balkus, J.P. Ferraris, I.H. Musselman, Mixed-matrix membranes containing MOF-5 for gas separations, J. Membr. Sci. 328 (2009) 165–173.

[18] S. Kim, E. Marand, High permeability nano-composite membranes based on mesoporous MCM-41 nanoparticles in a polysulfone matrix, Microporous Mesoporous Mater. 114 (2008) 129-136.

[19] G. Schulz-Ekloff, J. Rathousky, A. Zukal, Mesoporous silica with controlled porous structure and regular morphology, Int. J. Inorg. Mater. 1 (1999) 97-102.

[20] N. Navascues, C. Tellez, J. Coronas, Synthesis and adsorption properties of hollow silicalite-1 spheres, Microporous Mesoporous Mater. 112 (2008) 561-572.

[21] M.J.B. Souza, A.S. Araujo, A.M.G. Pedrosa, B.A. Marinkovic, P.M. Jardim, E. Morgado, Textural features of highly ordered Al-MCM-41 molecular sieve studied by X-ray diffraction, nitrogen adsorption and transmission electron microscopy, Mater. Lett. 60 (2006) 2682-2685.

[22] C. Casado, J. Bosque, N. Navascues, C. Tellez, J. Coronas, Propane and 1,3,5-triisopropylbenzene single gas adsorption on hollow silicalite-1 spheres, Microporous Mesoporous Mater. 120 (2009) 69–75.

[23] D.P. Das, K.M. Parida, B.K. Mishra, A study on the structural properties of mesoporous silica spheres, Mater. Letters 61 (2007) 3942–3945.

[24] P.H. Pfromm, W.J. Koros, Accelerated physical aging of thin glassy polymer-films - evidence from gas-transport measurements, Polymer 36 (1995) 2379-2387.

[25] F. Li, Y. Li, T.S. Chung, S. Kawi, Facilitated transport by hybrid POSS®–Matrimid®–Zn^{2+} nanocomposite membranes for the separation of natural gas, J. Membr. Sci. 356 (2010) 14–21.

[26] Y. Zhang, K.J. Balkus, I.H. Musselman, J.P. Ferraris, Mixed-matrix membranes composed of Matrimid (R) and mesoporous ZSM-5 nanoparticles, J. Membr. Sci. 325 (2008) 28–39.

[27] S. Cheng, D.Z. Shen, X.S. Zhu, X.G. Tian, D.Y. Zhou, L.J. Fan, Preparation of nonwoven polyimide/silica hybrid nanofiberous fabrics by combining electrospinning and controlled in situ sol-gel techniques, Eur. Polym. J. 45 (2009) 2767-2778.

[28] S. Kim, E. Marand, J. Ida, V.V. Guliants, Polysulfone and mesoporous molecular sieve MCM-48 mixed matrix membranes for gas separation, Chem. Mater. 18 (2006) 1149–1155.

[29] P. Kumar, J. Ida, V.V. Guliants, High flux mesoporous MCM-48 membranes: Effects of support and synthesis conditions on membrane permeance and quality, Microporous Mesoporous Mater. 110 (2008) 595–599.

[30] D.W. Lee, S.J. Park, C.Y. Yu, S.K. Ihm, K.H. Lee, Novel synthesis of a porous stainless steel-supported Knudsen membrane with remarkably high permeability, J. Membr. Sci. 302 (2007) 265–270.

[31] C. Liu, J. Wang, Z. Rong, Mesoporous MCM-48 silica membrane synthesized on a large-pore alpha-Al_2O_3 ceramic tube, J. Membr. Sci. 287 (2007) 6–8.

[32] T.B. Lewis, L.E. Nielsen, Dynamic mechanical properties of particulate-filled composites, J. Appl. Polym. Sci. 14 (1970) 1449-1470.

[33] M. Moaddeb, W.J. Koros, Gas transport properties of thin polymeric membranes in the presence of silicon dioxide particles, J. Membr. Sci. 125 (1997) 143–163.

[34] T.C. Merkel, Z. He, I. Pinnau, B.D. Freeman, P. Meakin, A.J. Hill, Sorption and transport in poly (2,2-bis(trifluoromethyl)- 4,5-difluoro-1,3-dioxole-co-tetrafluoro-ethylene) containing nanoscale fumed silica, Macromolecules 36 (2003) 8406–8414.

[35] C. Joly, M. Smaihi, L. Porcar, R.D. Noble, Polyimide-silica composite materials: How does silica influence their microstructure and gas permeation properties?, Chem. Mater. 11 (1999) 2331-2338.

[36] T.L. Chew, A.L. Ahmad, S. Bhatia, Ordered mesoporous silica (OMS) as an adsorbent and membrane for separation of carbon dioxide (CO_2), Adv. Colloid Interface Sci. 153 (2010) 43-57.

[37] A. Bos, I.G.M. Pünt, M. Wessling, H. Strathmann, CO_2-induced plasticization phenomena in glassy polymers, J. Membr. Sci. 155 (1999) 67-78.

[38] R. Pal, Permeation models for mixed matrix membranes, J. Colloid Interface Sci. 317 (2008) 191-198.

[39] J.A. de Sales, P.S.O. Patrício, J.C. Machado, G.G. Silva, D. Windmöller, J. Membr. Sci. 310 (2008) 129–140.

Table 1. Comparison of XRD results of pure polymer (PSF and PI) and mixed matrix membranes with calcined MSSs.

Material	**2θ**	**d-spacing (Å)**
PSF	17.3º	5.2
16% MSS-PSF MMM	17.7º	5.0
PI	14.3º	6.2
16% MSS- PI MMM	14.8º	6.0

Table 2. Glass transition temperature (Tg) as a function of MSS mass fraction for MSS-PI MMMs.

wt.% MSS- PI MMM	Tg (°C)	Error
0	316.7	±1.8
4	323.7	±2.8
8	333.8	±2.2
16	343.8	±2.6

Table 3. Permeabilities and selectivities of MMMs including calcined MSSs and chemically extracted MSSs for equimolar H_2/CH_4 mixture at 35 ºC.

Sample	MSS treatment	Permeability (Barrer)		H_2/CH_4 Selectivity
		H_2	CH_4	
PSF	-	11.8	0.20	58.9
8% MSS-PSF MMM	calcined	26.5	0.34	79.2
	extracted	30.6	0.44	70.1
PI	-	30.4	0.23	132.4
8% MSS-PI MMM	calcined	46.9	0.29	164.4
	extracted	48.9	0.31	155.3

Table 4. Apparent activated energies of H_2, CH_4, CO_2 and N_2 for 0-16 wt % MSS- PI MMMs and 0-16 wt % MSS- PSF MMMs.

E_P (KJ/mol) / Sample	H_2	CH_4	CO_2	N_2
0% MSS- PI MMM	12.3	23.7	12.7	17.4
4% MSS-PI MMM	12.7	24.2	-	-
8% MSS-PI MMM	13.9	24.2	15.0	22.9
16% MSS-PI MMM	13.5	24.4	13.5	31.3
0% MSS- PSF MMM	14.0	24.7	-	-
4% MSS-PSF MMM	14.8	25.6	-	-
8% MSS-PSF MMM	19.8	29.7	-	-
16% MSS-PSF MMM	15.9	24.0	-	-

- not calculated in this work

Figures

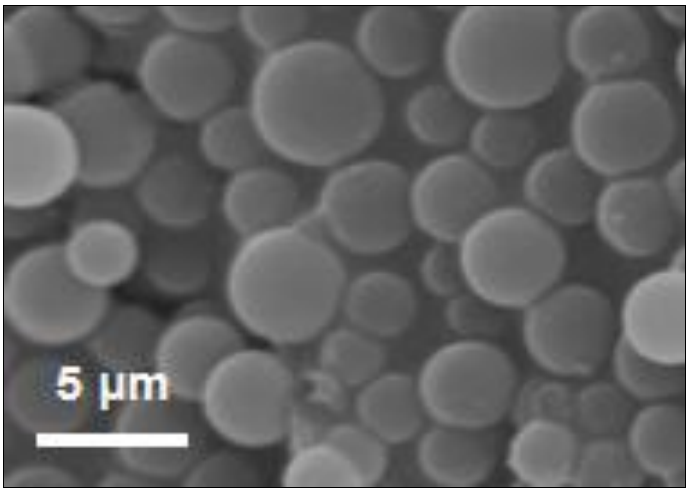

Fig. 1

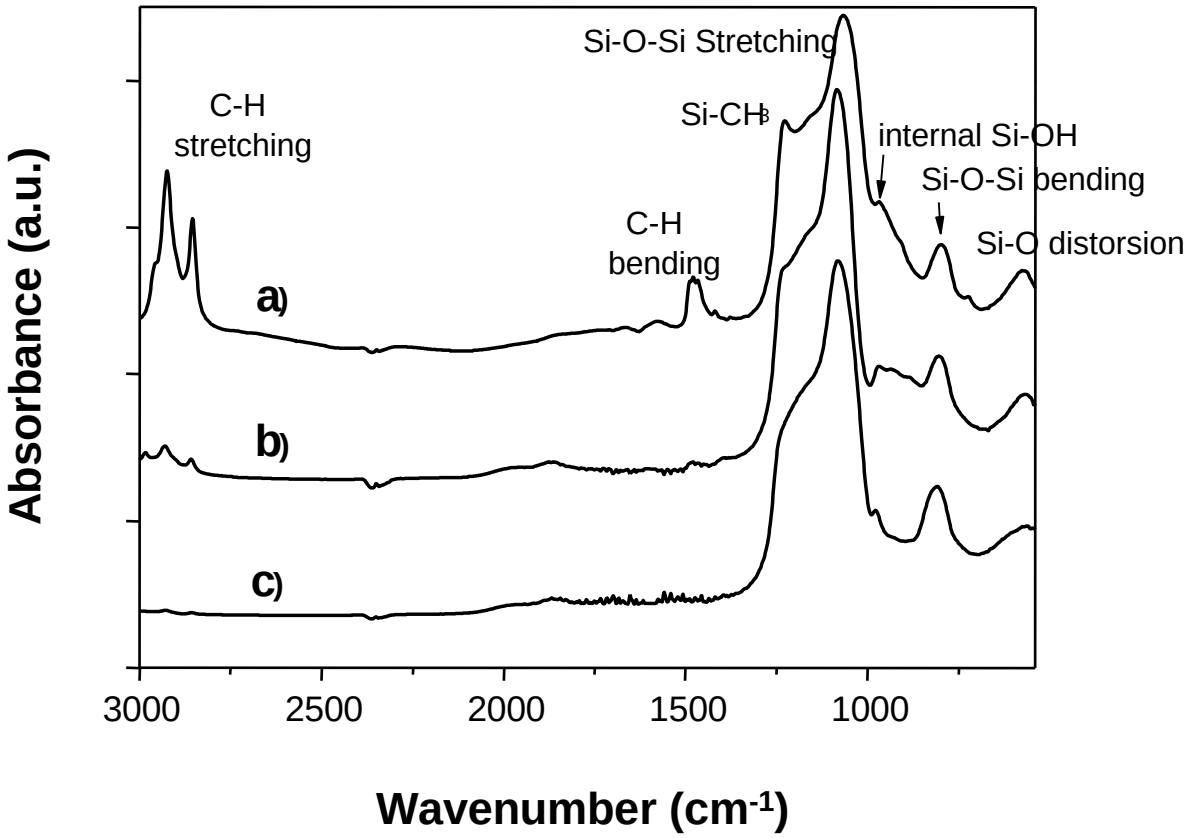
Si-O-Si Stretching
C-H
stretching
Si-CH3
internal Si-OH
Si-O-Si bending
C-H
bending
Si-O distorsion
a)
b)
c)
Absorbance (a.u.)
3000
2500
2000
1500
1000
Wavenumber (cm-1)

Fig. 2

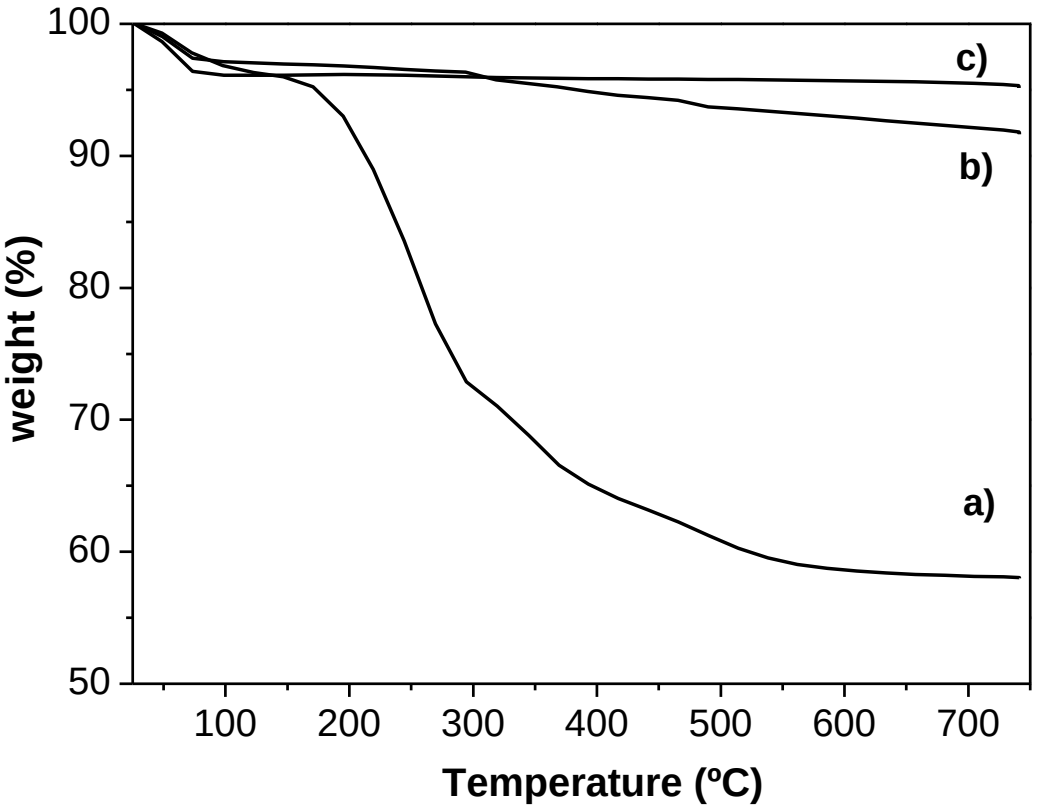
100
90
80
70
60
50
weight (%)
100
200
300
400
500
600
700
Temperature (ºC)
c)
b)
a)

Fig. 3

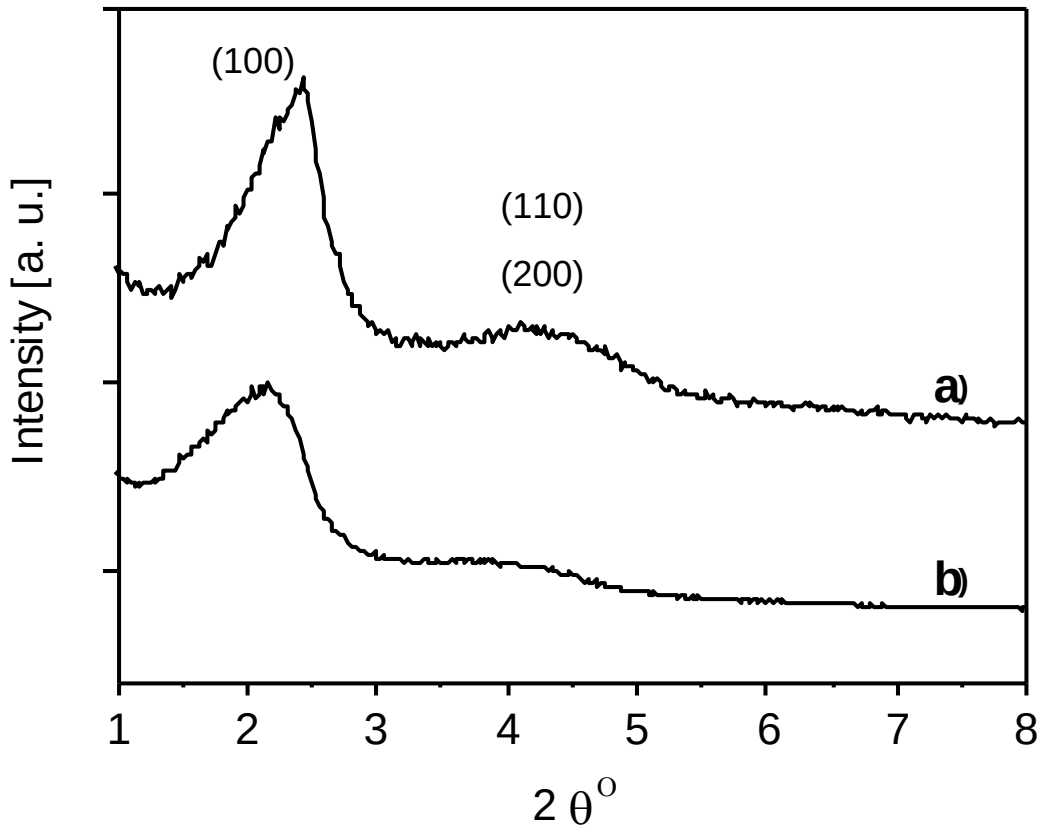

Fig. 4

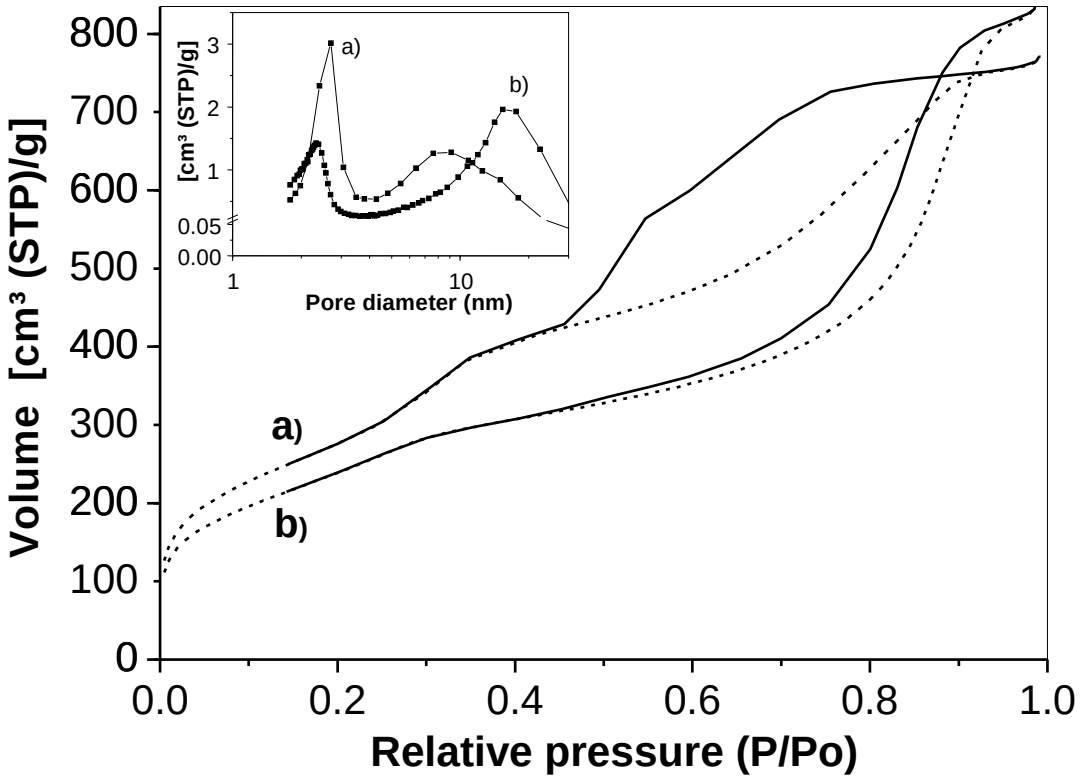
Volume [cm³ (STP)/g]
Relative pressure (P/Po)
a)
b)
[cm³ (STP)/g]
Pore diameter (nm)

Fig. 5

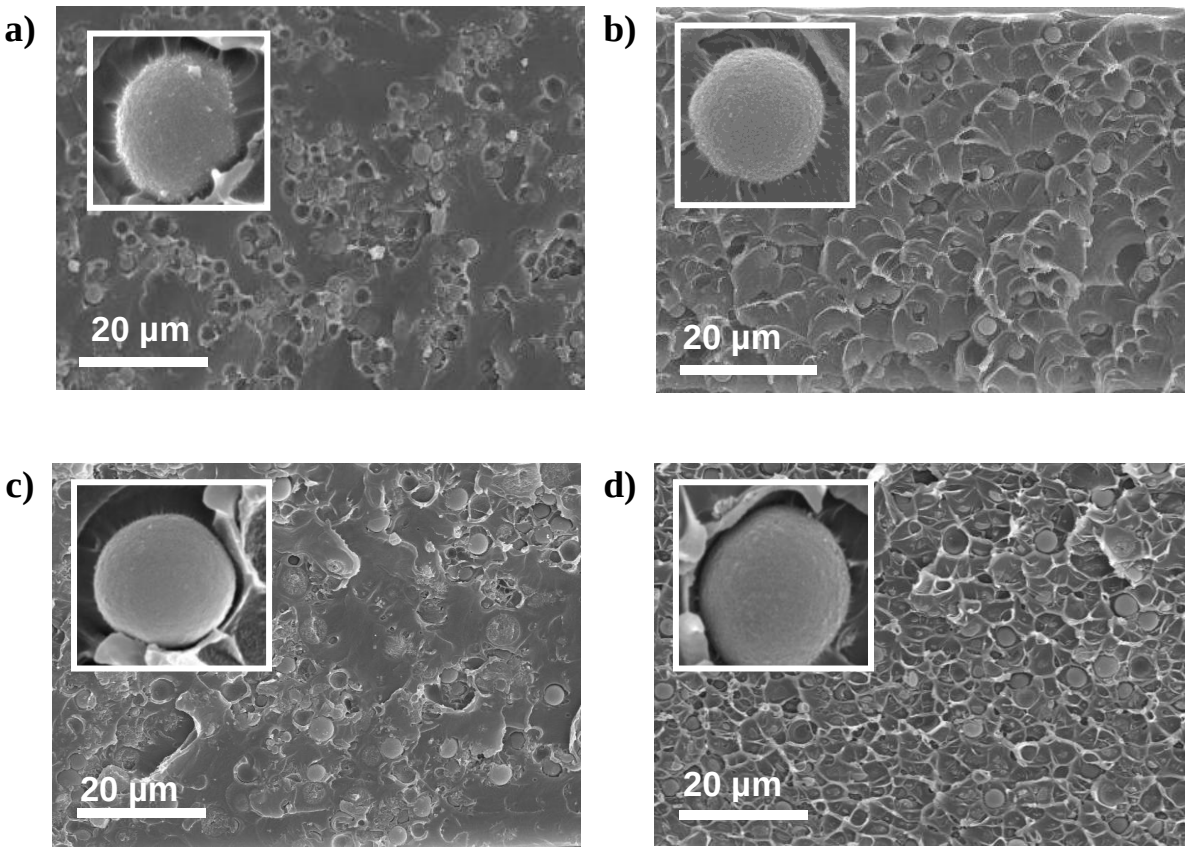

Fig. 6

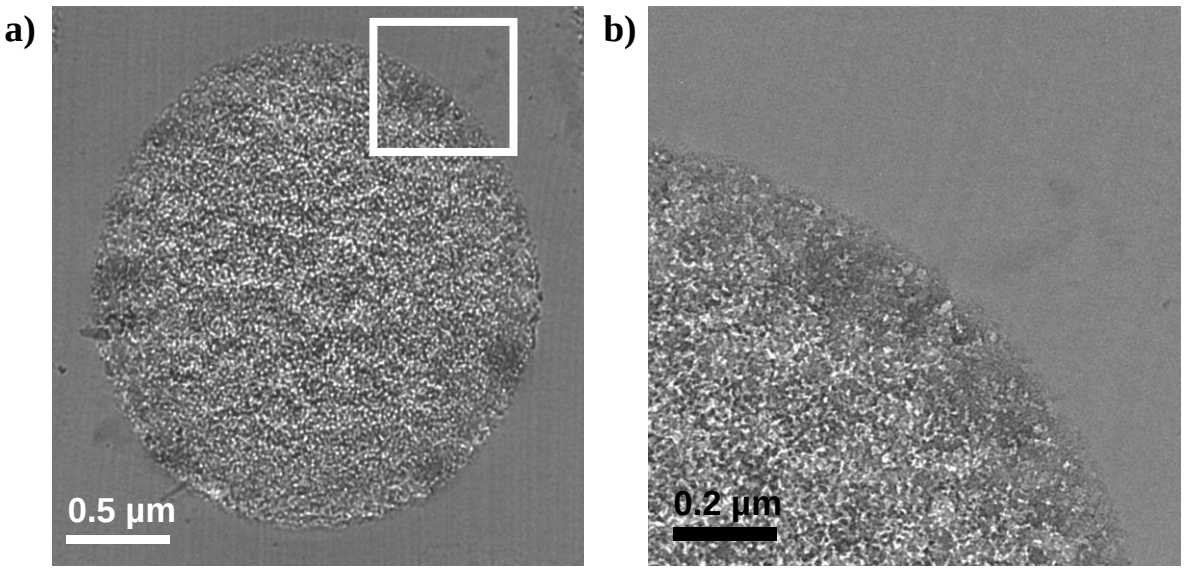

Fig. 7

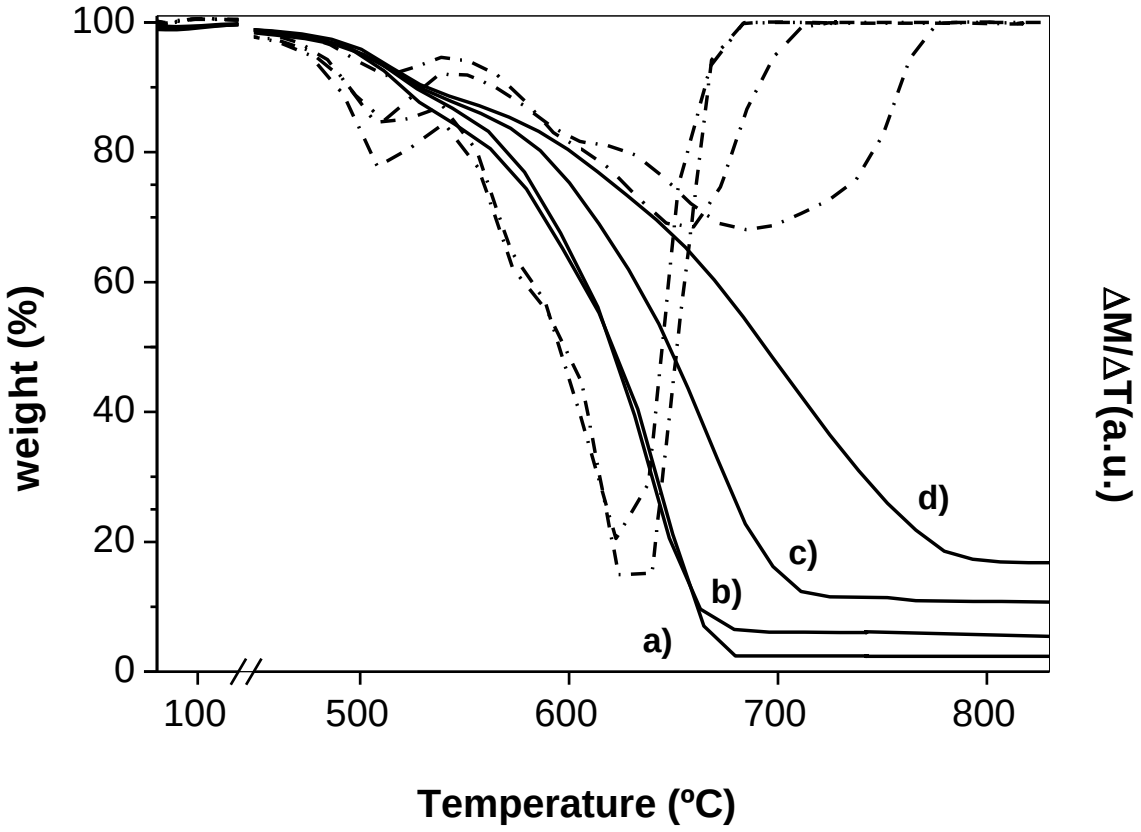
100
80
60
40
20
0
weight (%)
100
500
600
700
800
Temperature (°C)
ΔM/ΔT(a.u.)
a)
b)
c)
d)

Fig. 8

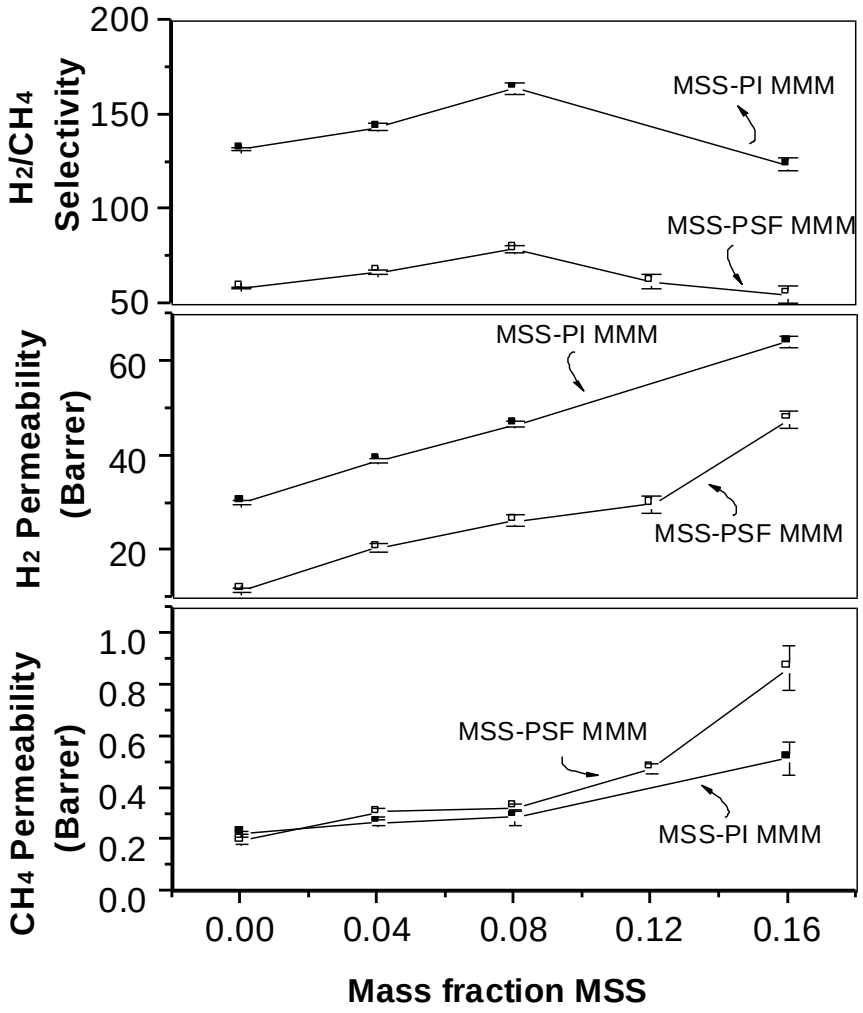
H2/CH4 Selectivity
200
150
100
50
MSS-PI MMM
MSS-PSF MMM
H2 Permeability (Barrer)
60
40
20
MSS-PI MMM
MSS-PSF MMM
CH4 Permeability (Barrer)
1.0
0.8
0.6
0.4
0.2
0.0
MSS-PSF MMM
MSS-PI MMM
0.00
0.04
0.08
0.12
0.16
Mass fraction MSS

Fig. 9

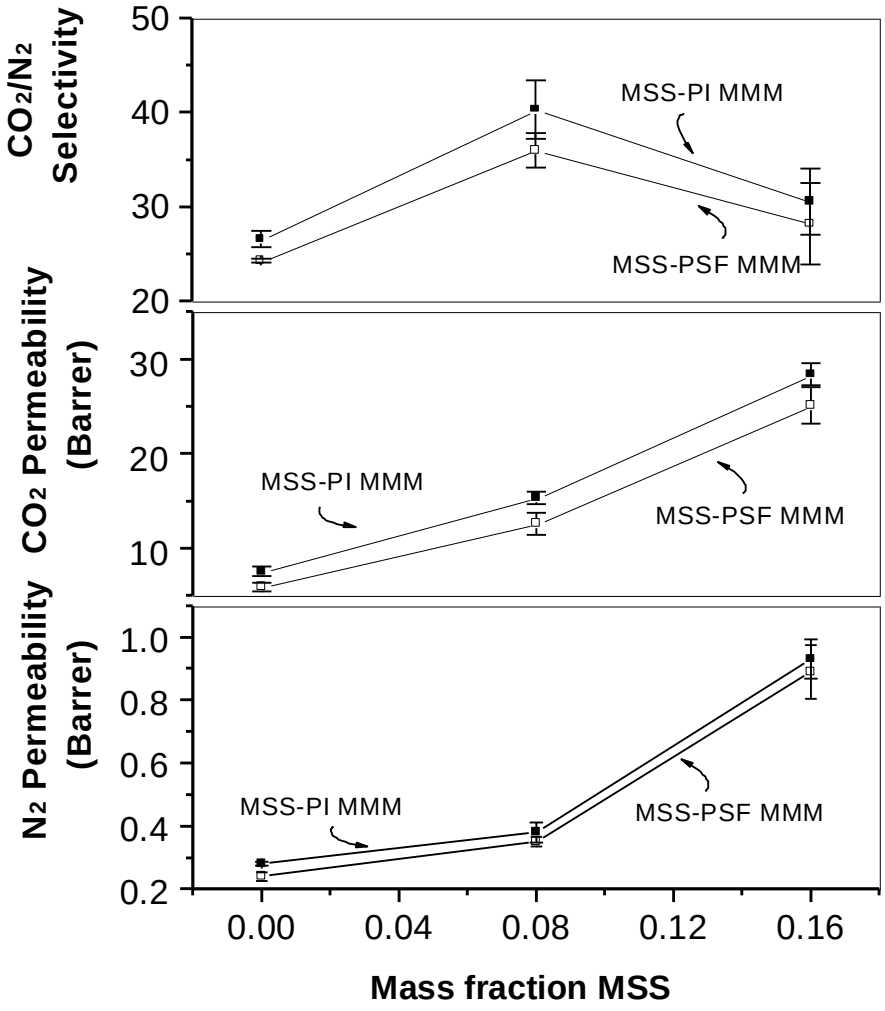
CO2/N2 Selectivity
50
40
30
20
MSS-PI MMM
MSS-PSF MMM
CO2 Permeability (Barrer)
30
20
10
MSS-PI MMM
MSS-PSF MMM
N2 Permeability (Barrer)
1.0
0.8
0.6
0.4
0.2
MSS-PI MMM
MSS-PSF MMM
0.00
0.04
0.08
0.12
0.16
Mass fraction MSS

Fig. 10

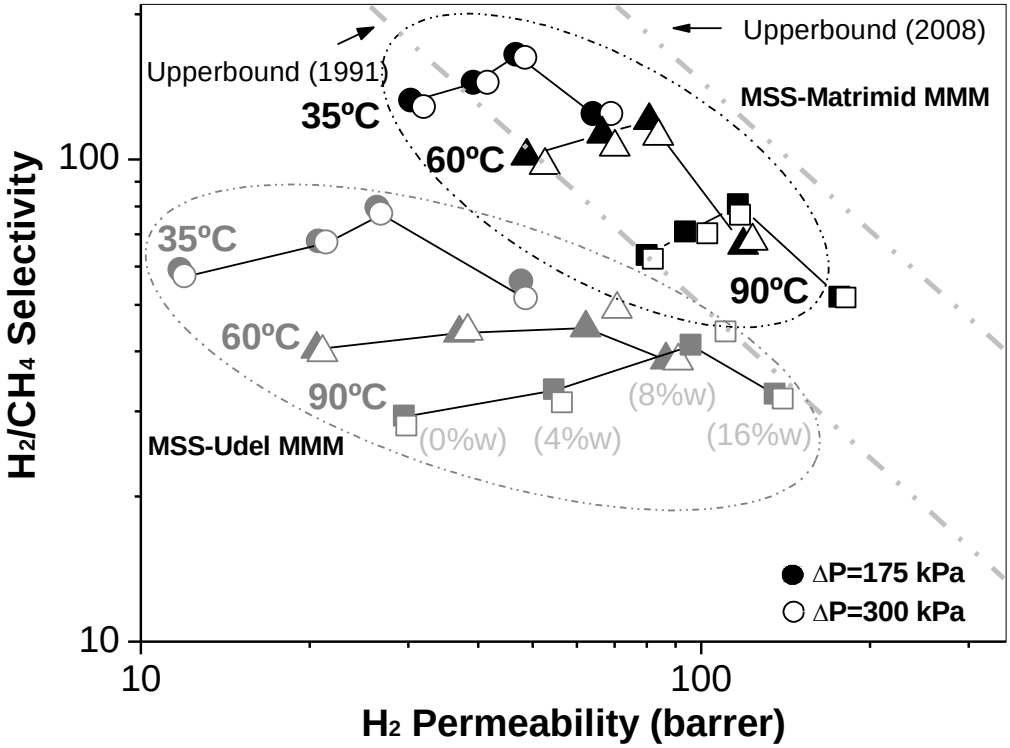
Upperbound (2008)
Upperbound (1991)
MSS-Matrimid MMM
35ºC
60ºC
90ºC
35ºC
60ºC
90ºC
(8%w)
(0%w)
(4%w)
(16%w)
MSS-Udel MMM
ΔP=175 kPa
ΔP=300 kPa
100
10
10
100
H2/CH4 Selectivity
H2 Permeability (barrer)

Fig. 11

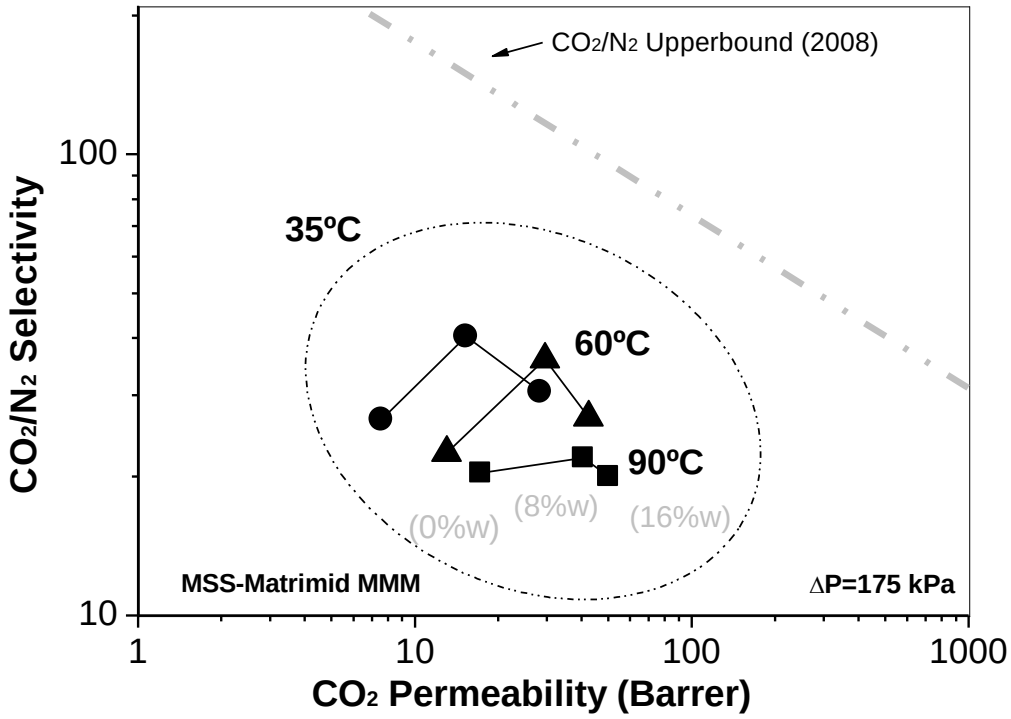
CO2/N2 Upperbound (2008)
35ºC
60ºC
90ºC
(0%w)
(8%w)
(16%w)
MSS-Matrimid MMM
ΔP=175 kPa
CO2/N2 Selectivity
CO2 Permeability (Barrer)
100
10
1
10
100
1000

Fig. 12

FIGURE CAPTIONS

Fig. 1. SEM image of the prepared mesoporous silica spheres

Fig. 2. FTIR spectra of: a) as-made MSSs at room temperature, b) chemically extracted MSSs at 110 ºC, c) calcined MSSs at 110.

Fig. 3. TGA weight losses versus temperature for a) as-made MSSs, b) chemically extracted MSSs, c) calcined MSSs.

Fig. 4. Low angle X-ray diffraction of MSSs: a) calcined b) chemically extracted.

Fig. 5. Nitrogen adsorption (dotted lines) and desorption (solid lines) isotherm branches for: a) calcined MSSs, b) chemically extracted MSSs. The inset represents the pore size distribution for calcined and extracted MSSs, respectively.

Fig. 6. Cross section SEM images of MMMs containing 8 wt % calcined MSS in: a) polysulfone matrix, b) polyimide matrix and 8 wt % chemically extracted MSS in: c) polysulfone matrix, d) polyimide matrix.

Fig. 7. TEM image of a): a calcined MSS within PI phase, b) detail of a).

Fig. 8. TGA loss weight and its derivatives versus temperature for 0, 4, 8 and 16 wt % of calcined MSS in PI matrix (curves a), b), c) and d), respectively).

Fig. 9. Gas permeation results for calcined MSS-PSF/PI with loadings in the range of 0-16 wt % for the equimolar mixture H_2/CH_4 tested at 35 ºC and ΔP=175 kPa. The data are average values of at least three membranes and error bar corresponds to standard deviation.

Fig. 10. Gas permeation results for calcined MSS-PSF/PI with loadings in the range of 0-16 wt % for the equimolar mixture CO_2/N_2 tested at 35 ºC and ΔP=175 kPa. The data

are average values of at least three membranes and error bar corresponds to standard deviation.

Fig. 11. Results for H_2/CH_4 at different pressures (ΔP of 175 kPa (closed symbols) and 300 kPa (open symbols)) and temperatures (at 35º C (circles), 60º C (triangles) and 90º C (squares)) within the Robesons'upper bound for MMMs composed of calcined MSS-PSF (0, 4, 8 and 16 wt %) and calcined MSS-PI (0, 4, 8 and 16 wt %).

Fig. 12. Results for CO_2/N_2 at fixed pressure and different temperatures (35º C (circles), 60º C (triangles) and 90º C (squares)) and ΔP=175 kPa within the Robesons´upper bound for calcined MSS-PI MMMs (0, 8 and 16 wt %).